ANNALES DE L'I. H. P., SECTION A

XU-SHENG ZHANG
FRANCO VIVALDI

Small perturbations of a discrete twist map

Annales de l'I. H. P., section A, tome 68, nº 4 (1998), p. 507-523
<http://www.numdam.org/item?id=AIHPA_1998__68_4_507_0>

Ann. Inst. Henri Poincaré,

Vol. 68, n° 4, 1998, p. 507-523. *Physique théorique*

Small perturbations of a discrete twist map

by

Xu-Sheng ZHANG* and Franco VIVALDI

School of Mathematical Sciences,
Queen Mary and Westfield College,
Mile End Road, London E1 4NS, England
E-mail: f.vivaldi@qmw.ac.uk.

ABSTRACT. – We investigate numerically a one-parameter family of twist mappings acting on a discrete lattice on the two-dimensional torus, and subject to a perturbation whose magnitude has the same size as the lattice spacing. These maps mimic the effects of (invertible) round-off errors on the orbits of an integrable twist map. We explore resonant and non-resonant behaviour in the limit of small lattice spacing, and find a dynamics rich in arithmetical and statistical features. © Elsevier, Paris

Key words: hamiltonian chaos, discrete twist map, round-off errors, periodic orbits, complexity.

RÉSUMÉ. – Nous étudions numériquement une famille à un paramètre d'applications « twist » intégrable. Nous explorons les comportements résonnants et non résonnants, dans la limite des petites mailles, et nous exhibons des comportements dynamiques riches tant du point de vue arithmétique que statistique. © Elsevier, Paris

1. INTRODUCTION

The study of hamiltonian systems with discrete phase space has been the focus of research for many years. Following the pioneering work of

* Permanent address: Centre for Nonlinear Complex Systems, Yunnan University, Kunming 650091, Yunnan, P.R. China.

Rannou [15], discretization has been introduced for the most varied reasons: to mimic quantum effects in classical systems [5], to achieve invertibility in a delicate numerical experiment [8], to characterize hamiltonian chaos arithmetically [14, 1, 6], to explore various phenomena connected to numerical orbits [9, 16, 7, 17, 11, 13].

An important property of all the hamiltonian systems mentioned above, is that discretization was performed in such a way as to retain invertibility. This requirement is necessary for consistency with symplectic geometry, in the sense that an invertible discretized system can be viewed as the restriction to a discrete set of some simplectic map of the continuum, although not necessarily of the original one. (Dissipative discrete representations of symplectic maps have also been considered, mainly in the context of round-off errors [2, 18, 10].)

In the simplest instances, discretizing amounts to restricting a continuum system to an invariant discrete set, in which case invertibility is achieved automatically. More often however, one truncates real coordinates. When this process preserves invertibility, one has a small canonical perturbation of the original continuum system, which generates fluctuations but no dissipation. Then, if the phase space is finite, all discrete orbits are periodic. If it is infinite, some orbits may escape to infinity in both time directions. The problem of stability under discretization is a prominent one, particularly if the continuum system is stable.

The present work is devoted to a numerical exploration of a family Φ_λ of invertible twist maps of the Chirikov-Taylor type [4], acting on a discrete doubly-periodic lattice $(\mathbf{Z}/N\mathbf{Z})^2$, which is obtained by reducing integer coordinates modulo a (large) integer N.

The maps are defined as follows

$$\begin{aligned} y_{t+1} &\equiv y_t + \epsilon_\lambda(x_t) \pmod N \\ x_{t+1} &\equiv x_t + y_{t+1} \pmod N \end{aligned} \tag{1}$$

with

$$\epsilon_\lambda(x) = \begin{cases} +1 & 0 \leq \{\lambda x\} < 1/2 \\ -1 & 1/2 \leq \{\lambda x\} < 1. \end{cases} \tag{2}$$

Here λ is a real number, and $\{\lambda x\}$ is the fractional part of λx. The perturbation function (2) has unit magnitude, and its dependence on x is periodic if λ is rational and quasi-periodic if λ is irrational. The effect of the perturbation is to displace the y-coordinate by the 'atomic' distance between lattice points. The invertibility of Φ_λ is easily verified.

Without perturbation, the map (1) is a linear integrable twist, which depends on the single parameter N, determining the coarseness of the discretization. In spite of its simplicity, the unperturbed system already possesses non-trivial features, which are found —for instance— in the asymptotics ($N \to \infty$) of some orbit-counting functions. One finds interesting scaling properties, together with fluctuations of arithmetical origin [13].

The functions ϵ_λ defined above have been chosen to satisfy three requirements: to have a bounded magnitude, to depend regularly on coordinates (the meaning of 'regular' will be clarified below), and to have a vanishing average

$$\lim_{N\to\infty} \frac{1}{N} \sum_{x=1}^{N} \epsilon(x) = 0.$$

These properties feature —for instance— in perturbations resulting from round-off errors, and we shall regard this as one motivation for the study of the above system (even though we make no claim that our system describes round-off errors realistically). In addition, ϵ_λ never vanishes, a property we have introduced in order to maximize the instabilities generated by such small perturbations. Independently from the round-off problem, the model (1) may also be viewed as a prototype for small nonlinear interaction on a lattice.

The information stored in the perturbing function ϵ_λ may be quantified by considering the number C_k of all possible k-subsequences of the doubly-infinite sequence $x \mapsto \epsilon_\lambda(x),\ x \in \mathbf{Z}$. The function C_k is sometimes referred to as the 'complexity' of the sequence. Regular and irregular behaviour in a sequence over a finite symbol space, is then associated to the growth rate of C_k being polynomial or non-polynomial in k, respectively. In our case, the complexity of $\epsilon_\lambda(x)$ is linear: $C_k \leq 2\,k$, for any choice of λ (cf. also[12]).

In this paper we explore two extreme regimes, corresponding to λ approaching zero (the 'most rational' number), and the golden mean (the 'most irrational' number), respectively. The former case will be dealt with in sections 2 and 3, where we consider the parameter values $\lambda = 1/N$, for large N. We find that the dynamics displays some familiar features of perturbed twist maps with divided phase space (Figure 1). In particular, these mappings may support stable librations at resonance, which form oval regions filled with periodic orbits. Their existence, size and detailed dynamics depend in a delicate manner on the rotation number, and on the discretization size N. Our main result is the arithmetical characterization

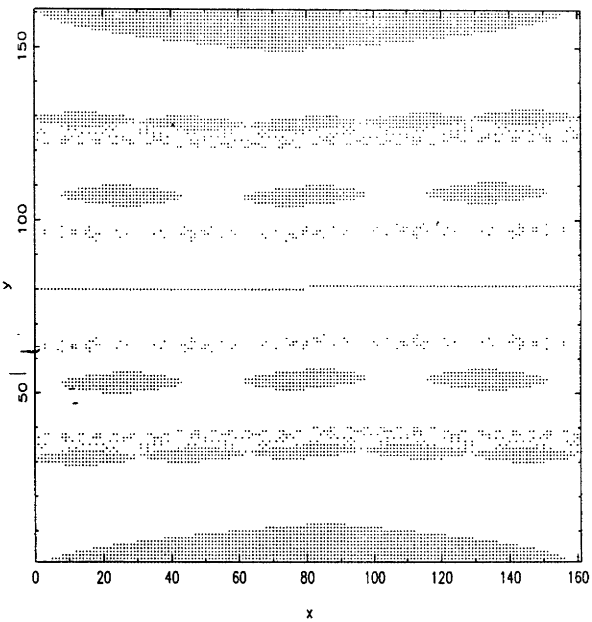

Fig. 1. – Phase portrait of the mapping (1) for $\lambda = 1/N$, and $N = 161$, showing several orbits. Some low-order rotation numbers support stable resonant regions (i.e., 0, 1/3, 1/5), while others do not (i.e., 2/5, 1/4). The invariant set at the rotation number 1/2, is a quasi-torus.

of such dependence, and the formulation of conditions for the stability of librations at resonance.

By contrast, the case of quasi-periodic perturbation ($\lambda = (1 + \sqrt{5})/2$) lacks geometrical features, and will be described statistically (see section 4).

We have analyzed numerically the growth of the period of the longest orbit on a given N-lattice, showing that in the limit of large N, such period grows quadratically, meaning that long orbits occupy a finite portion of the phase space.

The characterization of the transport in the 'action' variable y proved more difficult, due to large fluctuations and slow convergence. Nonetheless, we shall offer some evidence of the existence of a diffusion coefficient. Finally, we have estimated the complexity of the sequences $t \mapsto \epsilon(x_t) = y_{t+1} - y_t$, which determines the possible time-evolutions of the action. We find that initially the complexity grows exponentially $C_k = 2^k$, i.e., all sufficiently short binary subsequences are represented. The exponential growth is followed by an algebraic one after a 'breaktime', for which we have obtained some preliminary numerical estimates.

This work was partially supported by the UK Engineering and Physical Sciences Research Council under grant number GR/K 17026.

2. LOCAL MAPPINGS

In this section we consider the behaviour of the mapping (1) in correspondence to values of λ near zero (Figure 1). Letting $\lambda = 1/N$ in (2), we obtain a periodic ϵ-function, of period N, given explicitly by

$$\epsilon(x) = \epsilon_{1/N}(x) = \begin{cases} +1 & 0 \le x < \lfloor N/2 \rfloor \\ -1 & \lfloor N/2 \rfloor \le x < N \end{cases} \tag{3}$$

where $\lfloor \cdot \rfloor$ is the floor function. Here the periodicity of λ matches the periodicity of the lattice. This is done to minimize the total flux $\sum_{x=0}^{N-1} \epsilon(x)$, which would otherwise produce a net drift in y.

We consider the local behaviour of Φ^n in the vicinity of the m/n resonance, where m and n are coprime integers. From (1) we have

$$y_n \equiv y_0 + \sum_{t=0}^{n-1} \epsilon(x_t) \,(\text{mod}\, N) \qquad x_n \equiv x_0 + n y_0 + \sum_{t=0}^{n-1} (n-t)\epsilon(x_t)(\text{mod}\, N). \tag{4}$$

We define local coordinates

$$X = x - x^* \qquad Y = y - y^* \tag{5}$$

where x^* and y^* are to be determined. In what follows we shall assume that $n << N$, to ensure that the discretization is sufficiently fine to support motions near the resonances of order n. The analysis divides into three cases:

i) Elliptic-type behaviour. Let n be odd, and let $x^* = \lfloor N/2 \rfloor$. Then if $|X|$ is sufficiently small, we have $\sum_{t=1}^{n-1} \epsilon(x_t) = 0$, and from (4) and (5) we obtain

$$Y_n = Y_0 + \epsilon(x_0) \qquad X_n = X_0 + nY_n + \left(ny^* - \sum_{t=1}^{n-1} t\epsilon(x_t) \right).$$

There exists a unique integer y^* such that

$$0 \le ny^* - \sum_{t=1}^{n-1} t\,\epsilon(x_t) - mN < n \tag{6}$$

which corresponds to the m/n resonance, that is, $y^* \approx mN/n$. With such choice of y^* we obtain, after introducing the rescaled time $s = nt$ (the return time to a n-th order resonance)

$$\begin{aligned} Y_{s+1} &= Y_s - \operatorname{sign}(X_s) \\ X_{s+1} &= X_s + nY_{s+1} + \sigma \end{aligned} \qquad n \geq 1, \quad 0 \leq \sigma < n. \tag{7}$$

The shift σ, which depends on m, n and N, is the least non-negative solution to the congruence

$$\sigma(m, n, N) \equiv \Delta(m, n) - mN \pmod n \tag{8}$$

where

$$\Delta(m, n) = -\sum_{t=1}^{n-1} t\,\epsilon(x_t) = \sum_{t=1}^{n-1} t\,(-1)^{\lfloor 2mt/n \rfloor}. \tag{9}$$

From (9) we have

$$2m\Delta(m, n) = \sum_{t=1}^{n-1} 2mt\,(-1)^{\lfloor 2mt/n \rfloor} \equiv \sum_{s=1}^{n-1} 2s\,(-1)^{\lfloor 2s/n \rfloor} \pmod n \tag{10}$$

$$\equiv 2 \sum_{s'=1}^{(n-1)/2} s' - 2 \sum_{s'=1}^{(n-1)/2} \left(s' + \frac{n-1}{2} \right) \pmod n \tag{11}$$

$$\equiv - \sum_{s=1}^{(n-1)/2} (n-1) \equiv \frac{n-1}{2} \pmod n \tag{12}$$

where we have used the fact that if t runs through all non-zero residue classes modulo n, so does $s = mt$, since m is relatively prime to n, and then we have re-arranged the sum. Because n is odd, 2 has an inverse modulo n, and we have

$$\Delta(m, n) \equiv -(4m)^{-1} \pmod n \tag{13}$$

and finally, from (8)

$$\sigma(m, n, N) \equiv -(4m)^{-1} - mN \pmod n. \tag{14}$$

ii) Hyperbolic-type behaviour. Let n be odd. The choice $x^* = 0$ yields the local map for unstable motions

$$\begin{aligned} Y_{s+1} &= Y_s + \operatorname{sign}(X_s) \\ X_{s+1} &= X_s + nY_{s+1} + \sigma' \end{aligned} \qquad n \geq 1, \qquad 0 \leq \sigma' < n \tag{15}$$

where σ' is now given by

$$\sigma'(m,n,N) \equiv (4m)^{-1} - mN(\mathrm{mod}\, n). \tag{16}$$

iii) Parabolic-type behaviour. Let n be even. We have $\sum_{t=0}^{n-1} \epsilon_t = 0$, and proceeding as above we obtain

$$\begin{aligned} Y_{s+1} &= Y_s \\ X_{s+1} &= X_s + nY_{s+1} + \sigma \end{aligned} \qquad n \geq 1, \qquad 0 \leq \sigma < n \tag{17}$$

where σ is given by

$$\sigma(m,n,N) \equiv -\frac{1}{m}\left(\frac{n}{2}\right)^2 - mN(\mathrm{mod}\, n). \tag{18}$$

This time the local mapping describes the behaviour near, $x^* = \lfloor N/2 \rfloor + N/(2\,n)$.

We are interested in the instances in which the local dynamics may support *bounded* invariant sets, since the latter can be realized in the global mapping, by choosing N sufficiently large.

For hyperbolic-type motions (15), one verifies that all local orbits escape to infinity. This case is of little interest to us.

In the local parabolic mapping (17) all orbits escape if $\sigma > 0$, while for $\sigma = 0$ the entire X-axis is fixed. The corresponding global invariant set consists of n segments, joined at the boundary by (possibly) a step of unit magnitude in the y-direction. These invariant sets are the analogue of encircling invariant sets of the KAM type, and will be called *quasi-tori.* A quasi-torus can exist only when $\sigma = 0$, for otherwise the line of fixed points $Y = -\sigma/n$ does not occur at an integer value of Y, and therefore it is not realized on the integer lattice.

The richest dynamics is found in the local elliptic motions (7), which we shall study in the next section. A key local parameter is the shift σ, whose value depends on the global rotation number m/n as well as on the size N of the discretization, according to (14). The following result characterizes a sequence of lattices for which the correspondence between global and local dynamics is particularly simple.

PROPOSITION 1. – *Let n be odd. Then if N is any sufficiently large multiple of n, all n-order resonances of the mapping (1) have a distinct normal form, corresponding to all values of σ relatively prime to n.*

(The meaning of 'sufficiently large' will be discussed in the next section.)

The above result follows readily from (14). If n divides N, the equation $\sigma \equiv -(4m)^{-1} (\bmod n)$ has precisely one non-zero solution m for each choice of σ prime to n. In particular, if n is prime, then σ can be chosen arbitrarily. On the other hand, if n does not divide N, then in general the mapping $m \mapsto \sigma(m)$ is not invertible modulo n, so that the local dynamics at distinct rotation numbers may be the same. Each allowed value of σ will be realized for infinitely many values of N, corresponding to arithmetic progressions modulo n.

3. STRUCTURE OF DISCRETE RESONANCES

In this section we study the geometrical properties of the elliptic-type resonant motions of the local mapping (7). The main tool is the associated return mapping F of the non-negative X-axis, which is crossed repeatedly by every orbit. Such mapping is obtained as the composition of two transformations, $F = F_- \circ F_+$ carrying the orbit from non-negative values of X to negative ones, and vice-versa. We find

$$\begin{aligned} F_+(X) &= X + 2\,u_+\sigma - n\,u_+^2 \qquad\qquad X \geq 0 \\ u_+ &= \begin{cases} \lceil U_+ \rceil & U_+ \notin \mathbf{Z} \\ U_+ + 1 & U_+ \in \mathbf{Z} \end{cases} \\ U_+ &= \left(2\,\sigma - n + \sqrt{(2\,\sigma - n)^2 + 8\,n\,X}\right)/2\,n \end{aligned} \tag{19}$$

and

$$\begin{aligned} F_-(X) &= X + 2\,u_-\sigma + n\,u_-^2 \qquad\qquad X < 0 \\ u_- &= \lceil U_- \rceil \\ U_- &= \left(-\,2\,\sigma - n + \sqrt{(2\,\sigma + n)^2 - 8\,n\,X}\right)/2\,n \end{aligned} \tag{20}$$

where $\lceil \cdot \rceil$ is the ceiling function. Composition of the two mappings yields

$$X' = F(X) = F_-(F_+(X)) = X + 2\,\sigma(u_+ + u_-) + n(u_-^2 - u_+^2) \qquad X \geq 0. \tag{21}$$

For every n and σ, the half-way return maps $F_\pm$ are 'discontinuous', in the sense that they have unbounded variations $F_\pm(X+1) - F_\pm(X)$. There are infinitely many jumps, occurring in correspondence of the discontinuities of the ceiling function in (19) and (20). These jumps are the root cause of the complicated dynamics of discrete resonances.

We define the *index* $I(X)$ of a point X to be the period of the orbit of F at X. Thus a bounded orbit of (7) has finite index, while a capture-escape orbit has infinite index. The index is (essentially) the number of loops the orbit performs around the origin, although this concept is not well-defined in the vicinity of the origin ($0 \leq X < n - \sigma$).

When σ is equal to zero, one verifies that all orbits of (7) have index 1 (one has $u_- = u_+$ in (21)), that is, every point is a fixed point of the return mapping. Some orbits of this type are displayed in Figure 2 (left), for a resonance of order $n = 17$. The overall structure is regular, even though the dynamics is not entirely trivial. The orbits are placed asymmetrically with respect to the origin, and intersect each other.

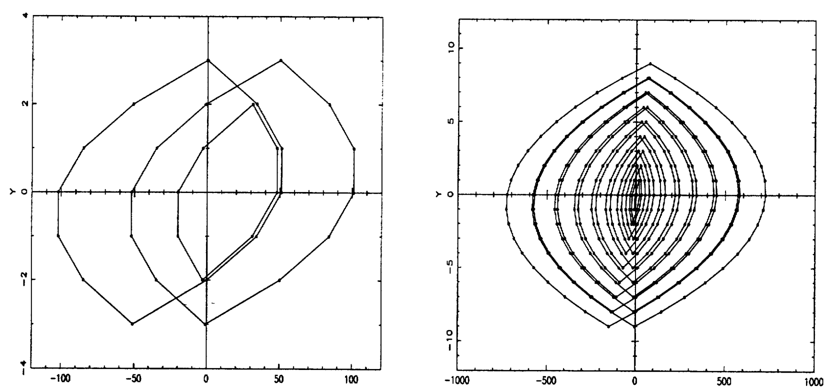

Fig. 2. – Elliptic-type orbits of the local mapping (7) for $n = 17$. *Left:* three orbits of unit index, corresponding to $\sigma = 0$. Note the discontinuous nature of the half-period function F_+, defined in (19). *Right:* a single orbit of index 17, for $\sigma = 4$.

The case of non-zero shift is more complicated (see Figure 2, right). The orbits typically have index greater than 1, and perform large radial excursions. Some of our findings on the behaviour of the index function are summarized in the following conjecture

CONJECTURE 1. – *If n is not divisible by 4, then the index of every orbit of the mapping (7) does not exceed n. Moreover, if n is prime, then, for all sufficiently large X, all orbits have index n.*

For the sake of completeness, we have included the case of even n, even though for such values the mapping (7) is not the local map of the original mapping (1) at resonance.

From the above conjecture it follows that when n is not divisible by 4, all orbits are bounded. The most interesting dynamics take place at resonances of prime order, for which the index eventually attains a limiting value (see Figure 2, right). The *(maximal) critical amplitude* characterizes the amplitude of librations at which the asymptotic regime sets in. It is defined as the largest integer Θ for which $I(\Theta) \neq n$. Likewise we define the *minimal critical amplitude* to be the smallest value of θ for which the index $I(\theta)$ is equal to n.

Critical amplitudes have a very irregular dependence on the order n of the resonance and on the value σ of the shift, although several features depend only on the ratio σ/n. The largest values of Θ (Figure 3, left) occur at the two primary peaks $\sigma/n \approx 1/4$, and $3/4$, which we have found to exist for every prime we have examined. The secondary peaks are located at $\sigma/n \approx a/4b$, for a and b coprime integers, but not all values of a and b do necessarily give rise to a peak, even when a and b are small (we call b the *order* of the peak). Moreover, the existence of a high-order peak at a given location was found to depend on n.

However, whenever a peak existed for a sufficiently large prime n, we verified the following scaling law:

$$\frac{b^2}{n^3}\,\Theta(na/4\,b) \approx \frac{1}{8}$$

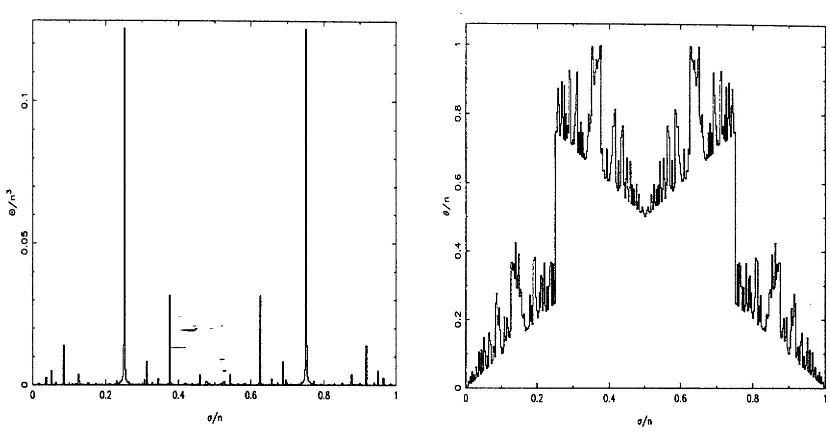

Fig. 3. – Critical amplitudes vs. shift for the resonances of prime order $n = 419$. All quantities are normalized. *Left:* Maximal amplitude. *Right:* Minimal amplitude.

suggesting the existence of a limiting value, to be taken along a suitable infinite sequence of prime values of n. A similarly irregular dependence on the shift is displayed by the minimal critical amplitude (Figure 3, right).

In the case of a large prime order n, and a value of the shift corresponding to the primary peaks of the critical amplitude, the normalized index $I(x)/n$ reveals a comb-like structure, shaped by a smooth envelope (Figure 4). Each tooth in the comb corresponds to points whose index is not maximal. We believe that this envelope reaches a limit functional form, which is independent of the prime chosen, and which describes the universal pre-asymptotic behaviour of resonances of large prime order.

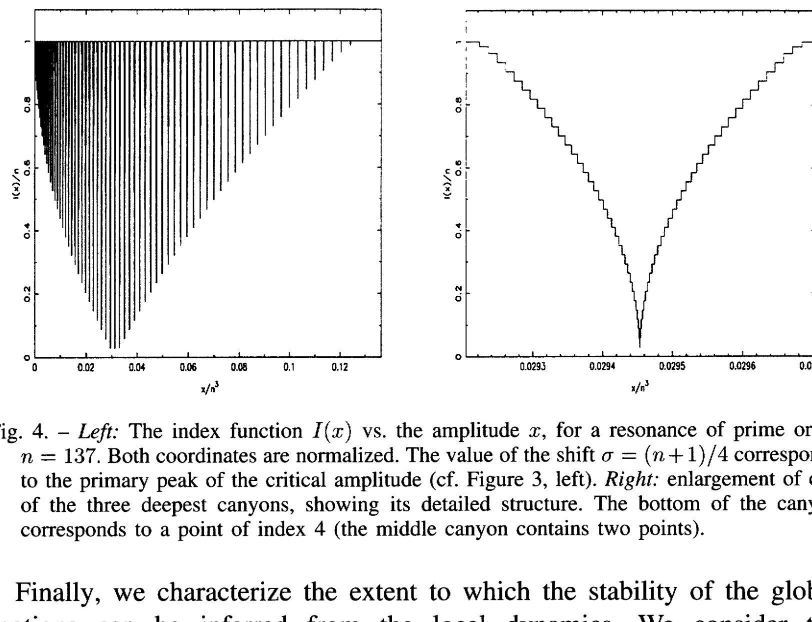

Fig. 4. – *Left:* The index function $I(x)$ vs. the amplitude x, for a resonance of prime order $n = 137$. Both coordinates are normalized. The value of the shift $\sigma = (n+1)/4$ corresponds to the primary peak of the critical amplitude (cf. Figure 3, left). *Right:* enlargement of one of the three deepest canyons, showing its detailed structure. The bottom of the canyon corresponds to a point of index 4 (the middle canyon contains two points).

Finally, we characterize the extent to which the stability of the global motions can be inferred from the local dynamics. We consider the intersection of a local invariant set with the X axis, and define its *radius* to be the absolute value of the point of this set which is furthest from the origin. Let $\Omega(X)$ be the largest invariant set of radius not exceeding X. We associate to $\Omega(X)$ two positive integers, namely its *(outer) radius* $R(X) = R(\Omega(X))$, and its *inner radius* $r(X)$, the latter being the radius of the largest interval enclosing the origin, which is contained in $\Omega(X)$.

Translating the above definitions in terms of global dynamics, we conclude that the largest invariant set which is contained in the central island of the m/n resonance (for odd n), and which has a local counterpart, has radius not exceeding $R(N/2n)$ (measured from the centre of the island). Points located futher away will not evolve according to the local map, and are expected to escape from the neighbourhood of the resonance. By the same token, the closest approach to the centre of the island for an orbit non describable in local terms is given by $r(N/2n)$.

In Figure 5 we display the X-dependence of outer and inner radii, for some resonances of prime order $n = 11$. The behaviour is step-like, with an overall linear growth. For $\sigma = 0$, we have $R(X) \sim r(X) \sim X$, which explains the large size and regular boundary of resonances of this type. An example is given by the resonances appearing in Figure 1, for which $\sigma = 0$, from formula (14). When the shift is non-zero, we typically have $r(X) < R(X)$, and the inner radius's growth rate is strongly dependent on the resonance parameters. One finds $r(X) = 0$ for $X < \Theta(n, \sigma)$, and moreover the growth rate of r decreases with increasing critical amplitude. Thus the larger the critical amplitude, the deeper an orbit can penetrate inside a resonant domain.

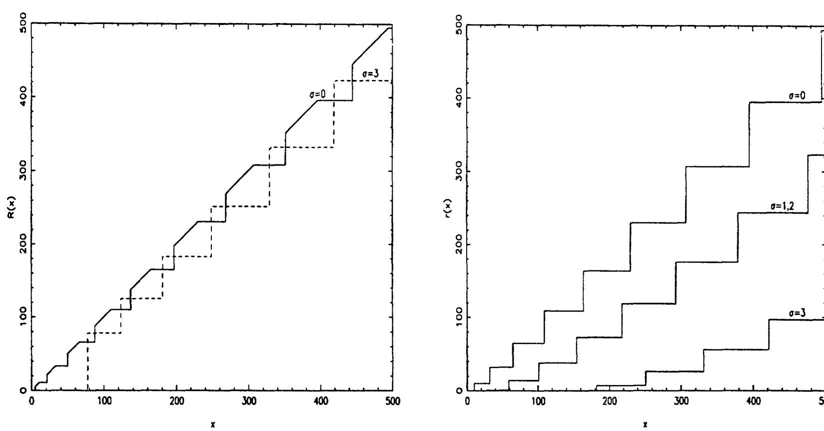

Fig. 5. – Dependence of the radii of maximal invariant set on the amplitude, for some resonances of prime order $n = 11$. *Left:* Outer radius $R(X)$ for $\sigma = 0$ and 3. *Right:* Inner radius $r(X)$, for $\sigma = 0, \ldots, 3$.

4. A QUASI-PERIODIC PERTURBATION

In this section we consider the case in which the perturbation ϵ_λ is quasi-periodic, in correspondence to the golden mean parameter value $\lambda = (1 + \sqrt{5})/2$.

We begin by addressing the problem of periodicity. For each $N \geq 1$, let $T = T(N)$ be the period of the longest periodic orbit of Φ on the $N \times N$ lattice. As a rule, functions of this type feature very large fluctuations

[9, 3, 17], and ours is no exception. A logarithmic plot of $T(N)$ is displayed in Figure (6) (top).

The lower envelope is linear. The upper envelope is quadratic, with coefficient very close to unity $(0.92\ldots)$ indicating that the orbits with maximal period invade a large portion of the phase space. To suppress fluctuations, we consider the average order $\langle T\rangle$ of T, given by

$$\langle T\rangle(N) = \frac{1}{N}\sum_{k\leq N} T(k) \tag{22}$$

which is represented by a thick solid curve. In Figure (6) (bottom) we plot its normalized value. Comparison between domain and range shows that, asymptotically, $\langle T\rangle$ is dominated by a quadratic term, although the persisting fluctuations are (at best) a warning of slow convergence.

Next we consider the time-evolution of the action

$$y_t - y_0 = \sum_{k=0}^{t-1} \epsilon(x_k)$$

in the limit of large N. The main question concerns the existence of a diffusion coefficient, that is, the long-time limit of the normalized variance

$$D(t) = \frac{1}{t}\,\langle (y_t - y_0)^2\rangle$$

where the average is computed over all points of a sufficiently long orbit. The results of Figure 7 were computed using three distinct orbits, each of period greater than 10^5, and each occupying at least 30% of the phase space. In spite of the large size of the averaging sample, the dependence of D on the choice of the orbit remains considerable. These data are consistent with the existence of a diffusion coefficient, but the large fluctuations prevent us from making any firm speculation. It is worth noting that the relaxation times of $D(t)$ are here much longer that those observed for round-off diffusion in a *linear* planar rotations [17].

We finally address the problem of determining the growth rate of the complexity C_k of the sequence $t \mapsto \epsilon(x_t)$, as computed along orbits of sufficiently long period.

For comparison, let us first consider the complexity C_k for the doubling map on the circle, with the usual binary symbolic dynamics. The orbits of maximal period $T = N - 1$ occur on certain prime lattices N (determined by the condition that 2 be a primitive root modulo N). These orbits enjoy a

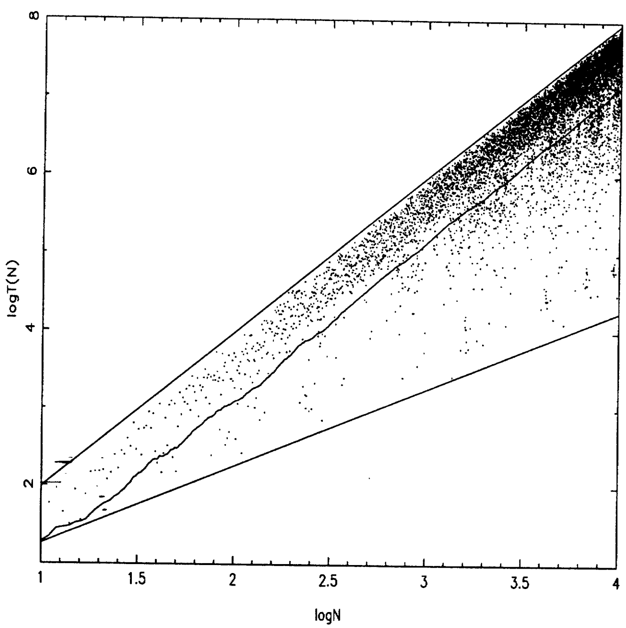

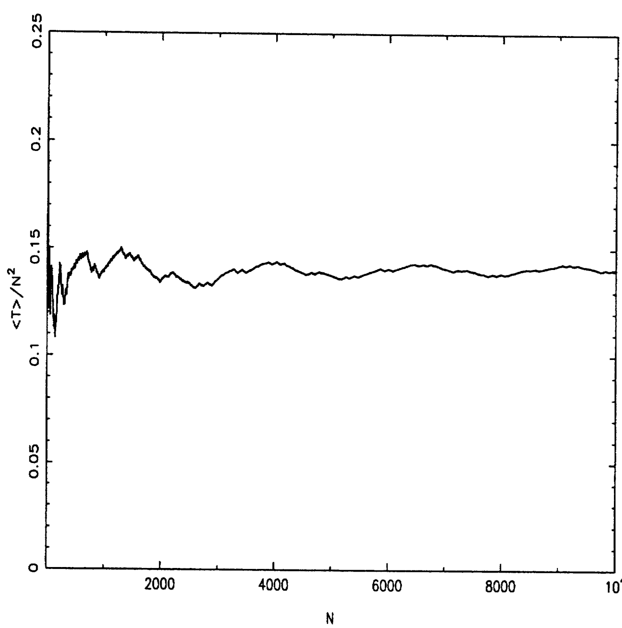

Fig. 6. – Maximal period of the orbits, on a lattice of size N, for the golden mean rotation number. *Top:* the period function $T(N)$, with upper and lower envelopes, and its average order $\langle T \rangle$. *Bottom:* normalized average order $\langle T(N) \rangle / N^2$.

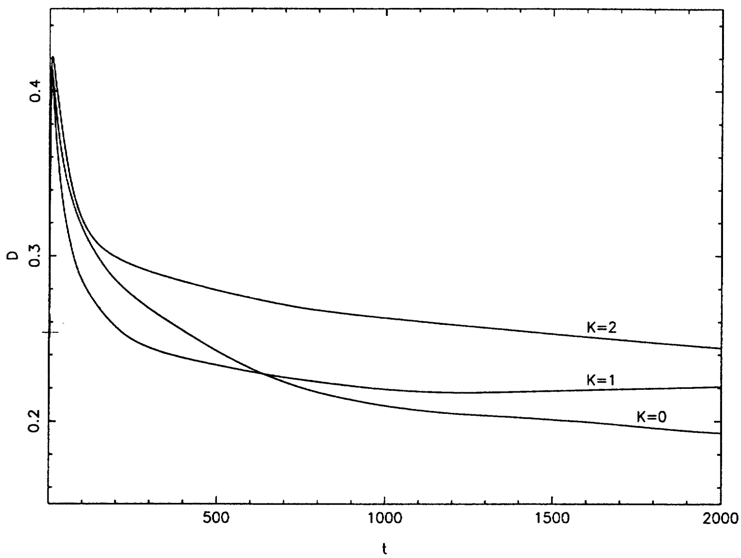

Fig. 7. – Time-dependence of the diffusion coefficient of the process $y_t - y_0$, computed along three different orbits. The quantity K, is defined as $K = (y_T - y_0)/N$ represents the number of times the orbit has wrapped around the torus in the y-direction.

complete uniformity in phase space, and support all subsequences of length k, for all k not exceeding $\lfloor \log_2(T+1) \rfloor$. We define the 'breaktime' $k^*(T)$ of a binary sequence of period T to be the largest positive integer k for which $C_k = 2^k$. We have

$$k^*(T) = \lfloor \log_2(T+1) \rfloor$$

independently from the initial condition (provided the latter is non-zero). For $k^* < k < T$, the complexity C_k grows slower than exponentially, to saturate to the value $C_k = T$ for $k \geq T$.

Returning to our mapping, the function C was computed using the longest orbit on each lattice. For small values of k, the complexity typically grows exponentially, $C_k = 2^k$, with all subsequences of length k appearing, roughly with equal frequency. After a breaktime $k^* = k^*(T(N))$, the exponential regime is followed by a polynomial one, which eventually saturates due to periodicity.

The scattered data in Figure 8 represent the breaktime computed for a large number of orbits of increasing period. For comparison, we also plot the average breaktime for the doubling map (solid line). The broken line is an average taken over several orbits of approximately the same period. In spite of large fluctuations, this results suggests that the breaktime

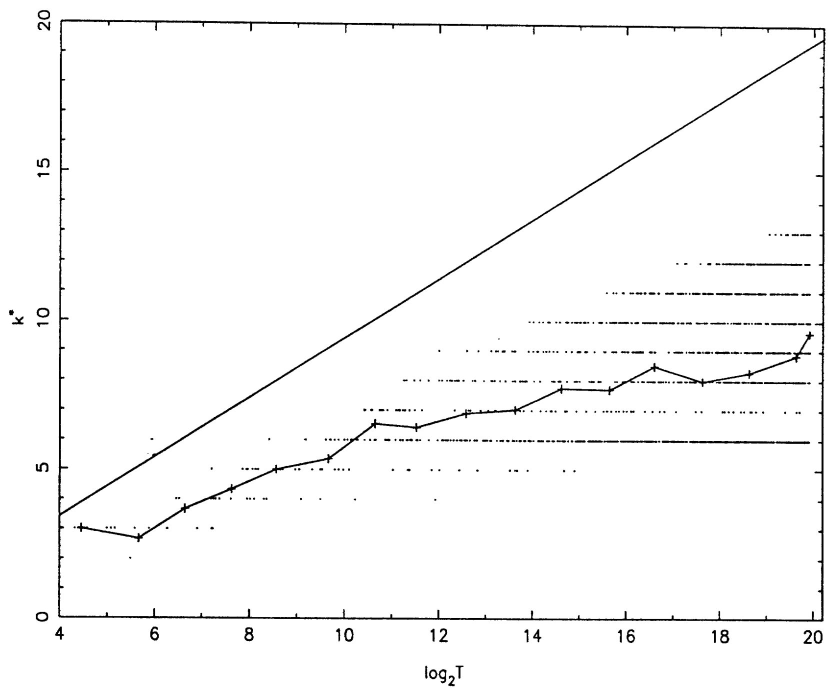

Fig. 8. – Breaktime for exponential growth of the complexity of the sequence $\epsilon(x_t)$, for the golden mean rotation number, and various orbits (scattered points). The broken line represents an average. The solid line is the breaktime for a pseudo-random sequence of the same length of the doubling map, for comparison.

grows slower than logarithmically, consistent with a picture of short time noise superimposed to long-time correlations. The question of whether k^* saturates to a limit value remains open.

REFERENCES

[1] M. Bartuccelli and F. Vivaldi, Ideal orbits of toral automorphisms, *Physica D*, Vol. **39**, 1989, pp. 194-204.

[2] M. Blank, Pathologies generated by round-off in dynamical systems, *Physica D*, Vol. **78**, 1994, pp. 93-114.

[3] C. Beck and G. Roepstoff, Effects of phase space discretization on the long-time behavior of dynamical systems, *Physica D*, Vol. **25**, 1987, pp. 173-180.

[4] B. V. Chirikov, A universal instability of many-dimensional oscillator systems, *Phys. Reports*, Vol. **52** (5), 1979, pp. 263-379.

[5] B. V. Chirikov, F. M. Izrailev and D. L. Shepelyansky, Dynamical stochasticity in classical and quantum mechanics, *Soviet Scientific Reviews C*, Vol. 2, Gordon and Breach, New York, 1981, pp. 209-267.

[6] M. Degli Esposti and S. Isola, Distribution of closed orbits for linear automorphisms of tori, *Nonlinearity*, Vol. **8**, 1995, pp. 827-842.

[7] D. J. D. EARN and S. TREMAINE, Exact numerical studies of hamiltonian maps: iterating without roundoff errors, *Physica D*, Vol. **56**, 1992, pp. 1-22.
[8] C. F. F. KARNEY, Long time correlations in the stochastic regime, *Physica D*, Vol. **8**, 1983, pp. 360-380.
[9] K. KANEKO, Symplectic cellular automata, *Phys. Lett. A*, Vol. **129**, 1988, pp. 9-16.
[10] V. KOZYAKIN, On finiteness of trajectories for one mapping associated with quasi-inversion of rotation mapping on integer planar lattice, preprint, Institute of Information Transmission Problems, Russian Academy of Sciences, Moscow, 1997. [kozyakin@ippi.ac.msk.su].
[11] J. H. LOWENSTEIN, S. HATJISPYROS and F. VIVALDI, Quasi-periodicity, global stability and scaling in a model of Hamiltonian round-off, *Chaos*, Vol. **7**, 1997, pp. 49-66.
[12] M. MORSE and G. A. HEDLUND, Symbolic dynamics II. Sturmian trajectories, *Amer. J. Math.*, Vol. **62**, 1940, pp. 1-42.
[13] D. NUCINKIS, D. K. ARROWSMITH and F. VIVALDI, Some statistical properties of discretized quasiperiodic orbits, *Nonlinearity*, Vol. **10**, 1997, pp. 1643-1674.
[14] I. C. PERCIVAL and F. VIVALDI, Arithmetical properties of strongly chaotic motions, *Physica D*, Vol. **25**, 1987, pp. 105-130.
[15] F. RANNOU, Numerical studies of discrete plane area-preserving mappings, *Astron. Astrophys.*, Vol. **31**, 1974, pp. 289-301.
[16] C. SCOVEL, On symplectic lattice maps, *Phys. Lett. A*, Vol. **159**, 1991, pp. 396-400.
[17] F. VIVALDI, Periodicity and transport from round-off errors, *Experimental Mathematics*, Vol. **3**, 1994, pp. 303-315.
[18] I. VLADIMIROV, Discretization of dynamical systems, preprint, Deakin University, Geelong, Victoria, 1996 [I. Vladimirov@mailbox.uq.edu.au].

(Manuscript received December 19, 1997;
Revised version received February 6, 1998.)